Elsevier Editorial System(tm) for International Journal of Mechanical Sciences
Manuscript Draft

Manuscript Number:

Title: Running Performance of an Aerodynamic Journal Bearing with Squeeze Film Effect

Article Type: Research Paper

Keywords: gas journal bearing, squeeze film, dynamic stability

Corresponding Author: Prof. Shigeka Yoshimoto,

Corresponding Author's Institution:

First Author: Shigeka Yoshimoto

Order of Authors: Shigeka Yoshimoto; Tomohiro Sho, BEng; Tadeusz Stolarski, PhD, DSc(Eng)

Abstract: Results of theoretical and experimental studies concerning the performance of an aerodynamic journal bearing which running is assisted by squeeze film ultrasonic levitation (SFUL) are presented in this paper. The SFUL mechanism not only can separate journal from the bearing at the start and stop phases of operation but also can significantly contribute to the dynamic stability of the bearing when it runs at speed. Computer calculations and validating experimental testing of a prototype device were carried out. It was found that that SFUL mechanism, when combined with aerodynamic lift, extends the threshold speed of bearing's instability by almost four times comparing to that of a bearing operating without SFUL. Typically, the bearing running without SFUL became unstable at the speed of 300 rpm while with the SFUL the speed at which instability became apparent was 10,000 rpm (calculated result) or 13,200 (experimental result).

Editor-in-Chief
International Journal of Mechanical Sciences

30th October 2012

Dear Editor,

On behalf of my co-authors I send to you for your consideration our paper entitled "Running Performance of an Aerodynamic Journal Bearing with Squeeze Film Effect".

I would be grateful to you for initiating due review process and letting me know it outcome.

Yours sincerely,

Professor Shigeka Yoshimoto

Tokyo University of Science

***Highlights (for review)**

Running Performance of an Aerodynamic Journal Bearing with

Squeeze Film Effect

Research highlights

The most important findings contained in the paper are:

1. Lightly loaded high-speed aerodynamic journal bearings are inherently unstable.

2. For applications requiring very high precision of motion this is a serious limitation for this type of bearings.

3. An innovative way of increasing running speed at which a bearing becomes unstable is proposed in the paper.

4. It is based on squeeze film ultrasonic levitation which mechanism is presented in the paper.

5. Both analytical and experimental results illustrating performance of the air journal bearing running without and with squeeze film ultrasonic levitation are presented.

6. Pressure generated by the squeeze film ultrasonic levitation has a very significant effect on the dynamic stability of the bearing as it is compatible with the pressure generated by aerodynamic mechanism.

7. Bearing operating with squeeze film ultrasonic had its instability speed increased more than thirty times comparing to that of the bearing running without squeeze film ultrasonic levitation.

Running Performance of an Aerodynamic Journal Bearing with Squeeze Film Effect

Tomohiro Sho, Shigeka Yoshimoto[1)]

Tokyo University of Science, Department of Mechanical Engineering,

1-14-6 Kudan-kita, 102-0073 Tokyo, Japan

yosimoto@rs.kagu.ac.jp

Tadeusz Stolarski

Brunel University, School of Engineering and Design, Uxbridge UB8 3PH,

United Kingdom

mesttas@brunel.ac.uk

Abstract

Results of theoretical and experimental studies concerning the performance of an aerodynamic journal bearing which running is assisted by squeeze film ultrasonic levitation (SFUL) are presented in this paper. The SFUL mechanism not only can separate journal from the bearing at the start and stop phases of operation but also can significantly contribute to the dynamic stability of the bearing when it runs at speed. Computer calculations and validating experimental testing of a prototype device were carried out. It was found that that SFUL mechanism, when combined with aerodynamic lift, extends the threshold speed of bearing's instability by almost four times comparing to that of a bearing operating without SFUL. Typically, the bearing running without SFUL became unstable at the speed of 300 rpm while with the SFUL the speed at which instability became apparent was 10,000 rpm (calculated result) or 13,200 (experimental result).

1) corresponding author

Keywords: gas journal bearing, squeeze film, dynamic stability

List of symbols

C_r radial bearing clearance

h air film thickness

f frequency of bearing's elastic deformations

f_y load on the bearing

m mass

N rotational speed of shaft

p air film pressure

r_0 nominal diameter of shaft

q_θ flow rate in circumferential direction

q_z flow rate in bearing's length direction

q_t flow rate due to squeeze action

t time

x_{cg} x coordinate of shaft centre

y_{cg} y coordinate of shaft centre

z coordinate along bearing's length

θ angular coordinate

ρ density

η viscosity

σ squeeze number

$\omega_1 = {}^{2\pi N}/_{60}$

$\omega_2 = 2\pi f$

1) corresponding author

1. Introduction

Ability to create a non-contact suspension of interacting objects has significant advantages in many situations and is of fundamental importance to the operation of mechanical systems. Being non-contact, the system can be operated at much higher speeds than using conventional mechanical bearings. Also contactless bearing system is practically free of overheating and wear thus it can run with high precision and high speed of motion.

Classical non-contact bearings, such as air bearings (both aerostatic and aerodynamic) and magnetic bearings are already used in a number of practical specialist applications. However, continuous supply of a large volume of clean air is required for the air bearings significantly increase the cost of their use. Additionally, external auxiliary devices (pumps, filters, piping) exclude this type of bearing from certain applications (clean room environment). Magnetic bearings cannot be used for magnetic sensitive configurations due to the strong magnetic flux. It is undoubtedly of great interest nowadays to find other concepts for realising contactless suspensions.

An acoustic wave can exert a force on objects immersed in the wave field. These forces are normally weak, but they can become quite large when using high frequency (ultrasonic) and high intensity waves. The forces can even be large enough to suspend substances against gravity force. This technique is called acoustic levitation. Since the sound waves used are often in the ultrasonic frequency range (higher than 20 kHz), it is more often called as ultrasonic levitation. Ultrasonic levitation has been firstly used for levitating small particles by creating a standing wave field between a sound radiator and a reflector, namely standing wave

1) corresponding author

ultrasonic levitation. Standing wave type ultrasonic levitators with various features were designed for applications in different scientific disciplines such as material processing and space engineering [1]. Another well-known type of ultrasonic levitation is squeeze film ultrasonic levitation. It happens when a flat surface is brought to a conformal radiation surface, which vibrates with high frequency.

As one of the promising ways to create a non-contact suspension, squeeze film ultrasonic levitation (SFUL) has been widely investigated for building non-contact linear and rotational bearings. In principle, squeeze film bearing should have most of the advantages of aerostatic bearings. Instead of pressurized air fed through orifice or porous material in aerostatic bearings, the load-carrying air film is generated by high frequency vibration and the corresponding squeeze action between two surfaces. Mechanism of the squeeze film pressure generation is schematically shown in Figure 1 and its analytical description can be found elsewhere [2]. External pressurized air supply is no longer needed. This feature allows the bearing interface to be as simple as two plain surfaces. The additional effort needed in this kind of bearing is to induce high frequency vibration in bearing surfaces. Several prototype non-contact suspension and transportation systems based on squeeze film levitation have been reported in the open literature. Seminal contributions to the analysis of squeeze film gas non-contact suspensions could be found elsewhere [3, 4, and 5].

In 1964, Salbu [6] first described the concept of constructing a non-contact bearing using squeeze film action. Salbu used magnetic actuators to generate the oscillation and the operating frequency was in the audible range, therefore the bearing was extremely noisy. In the later publications on squeeze film levitation, piezoelectric transducers in various shapes were commonly used to generate the squeeze action effectively. Several designs of squeeze film bearings using bulk piezoelectric

1) corresponding author

ceramics can be found in early U.S. patents filed in 1960s, invented by Warnock [7], Farron [8], and Emmerich [9]. These designs used bulky piezoelectric materials to create uniform vibration amplitude over the entire bearing surfaces. Therefore the transducers were rather massive and required high power to generate sufficient vibration amplitude. Scranton [10] suggested using bending piezoelectric elements to excite a flexural vibration mode of the bearing. This led to a very compact system design and much lower power dissipation. Wiesendanger [11] developed a linear guide using disc shape piezoelectric bending elements. The transducers were placed in the sliding part. The carriage which can move freely in a V-shaped rail made of two glass plates. Five disk shaped piezoelectric bending elements were mounted on the carriage. These elements directly constitute the bearing surface, resulting in a highly compact overall design.

Attempts to design aerodynamic bearing systems utilizing squeeze film levitation were undertaken and their results published [12, 13, and 14]. In one of them, the bearing shell was specially configured to secure its flexibility through the use of "elastic hinges" as shown in Figure 2. It could be elastically deformed with desired frequency by three piezoelectric actuators. During the start and stop phase of operation, the squeeze film pressure was developed and was sufficient to support even the stationary spindle. When the spindle reached appropriate rotational speed, the bearing system started to operate on aerodynamic principle without the need for acoustic levitation. This system was tested experimentally for low rotational speeds only and operated at rather low frequencies of vibration – hence the problem of excessive noise. Later on the bearing configuration was changed and piezoelectric actuators operating in ultrasonic range were deployed thus eliminating noise. The results of experimental testing of this improved journal bearing are presented

1) corresponding author

elsewhere [15]. However, the problem of simultaneous use of SFUL and aerodynamic effects for lightly loaded bearing systems running with ultra-high speed has never been systematically and purposefully investigated. It is, therefore, not known whether dynamics of an air bearing with light load acting on it can be controlled by pressure developed by SFUL. Also, it is desirable to find out whether the interaction between those two phenomena is synergic or not. An attempt to provide answers to these questions is presented in this paper.

2. Configuration of the bearing and its deformation modes

2.1 Geometry

The geometry and main dimensions of the bearing are shown in Figure 3. Both geometry and dimensions were arrived at on the basis of previous studies [15]. The bearing was made of aluminium (A2024) with 50 mm in length and 30 mm nominal bore diameter. Three different radial clearances were used, namely 10, 15, and 20 μm. The wall thickness was 3mm. Table 1 gives all important dimensions characterising the bearing while Figure 4 shows results of roundness measurements. Previous studies [15] clearly showed that the best material for bearing utilizing squeeze film ultrasonic levitation is aluminium as it has low coefficient of energy absorption. The bearing requires the use of three foil type PZTs (piezo-electric actuators) arranged around its circumference. The PZTs used were of rectangular shape of 12x10 mm and thickness of 0.5 mm and were attached to the bearing outer wall at specially machined flats, spaced by 120^{o}, with the help of special cement.

1) corresponding author

2.2 Deformation modes

In order to ascertain the magnitude of elastic deformation and to find out the shape of the bearing's bore in deformed state a computer modelling was carried out. In addition, computer simulation gave information concerning resonance frequencies and corresponding modes of elastic deformation for the bearing. This information allowed for the selection of a vibration frequency with highest amplitude at which a maximum acoustic pressure was anticipated to be generated. These were the main objectives of the computer simulation. A standard finite-element (FE) technique provided by ANSYS was used for this purpose. The shape and geometry of the bearing used for experimental testing ensured simplicity of machining which was also a factor to be taken into account if the bearing was considered for a practical application.

Figure 5 shows modes of elastic deformations of the bearing for five vibration frequencies as predicted by ANSYS while Figure 6 presents experimentally measured amplitude of elastic deformation of the bearing as a function of vibration frequency. It can be clearly seen that out of all recorded modes of elastic deformations the fifth mode, corresponding to the frequency of 58.2 kHz, produces the best, from squeeze pressure generation point of view, shape of the bore and largest elastic deformation (amplitude of 1.5 μm as shown in Fig.6).

Detailed examination of the geometry of the bearing in its deformed state (see Figure 5d) clearly show that a perfectly circular bore is transformed into a three-lobe geometry with three arcuate gaps created around the shaft. Because they are created cyclically therefore enable a pumping action, which can be analytically described in terms of the known squeeze mechanism [2]. Figure 7 shows elastic

1) corresponding author

deformation of the bore as a function of the position along the length (z-axis) and circumference (θ - angle) of the bearing. In particular, Figure 7a presents bearing deformation for three different positions along z-axis (0, 5 and 10 mm) and three θ angles equal to 0, 30 and 60 degrees. The largest deformation of the bore occurs at z = 10 mm and θ = 0 deg. Figure 7b shows deformation of the bore for z = 0 mm and a number of θvalues. It can be clearly ascertained that the largest deformation occurs at certain specific values of θ shown in the figure.

3. Theoretical analysis of performance

Figure 8 shows position of the shaft within the bearing together with important parameters characterising geometry of the system assumed for the construction of computer model of the bearing. Computer modelling of a bearing utilizing squeeze film ultrasonic levitation during operation requires inclusion in the Reynolds' equation the time dependent inertia effect. Owing to a very small thickness of the air film developed within the bearing, averaging the inertia effect of the film across its thickness is warranted. Differential form of the Reynolds' equation is obtained by integration of the continuity equation across the film thickness,

$$\frac{\partial q_x}{\partial x} + \frac{\partial q_y}{\partial y} + \frac{\partial (\rho h)}{\partial t} = 0 \qquad (1)$$

Where q_x and q_y are mass flow rates per unit length in Cartesian co-ordinate system. Using geometry and symbols from Figure 8, the following expression for the air film thickness can be derived,

1) corresponding author

$$h = C_r + x_{cg} sin\theta + y_{cg} cos\theta + c(\theta, z, t) \quad (2)$$

In eqn (2) the last term describes contribution to the air film thickness by cyclic elastic deformations of the bearing's bore. In general terms, this can be expressed by,

$$c(\theta, z, t) = A \times B \times \sin(2\pi f t) \quad (3)$$

Terms *A* and *B* in eqn (3) were estimated separately on the basis of data presented in Fig. 7. For example for $0 \leq \theta \leq 6$ term *A* was calculated from the expression: $A = -0.05\sin[\pi\frac{(\theta+6)}{12}]$, which particular form was provided by a curve fitted to experimental points (see Fig.7). Furthermore, for $6 \leq \theta \leq 114$, *A* was calculated from: $A = \sin[\pi\frac{(\theta-6)}{108}]$ and finally for $354 \leq \theta \leq 360$, *A* was obtained from: $A = -0.05\sin[\pi\frac{\theta-354)}{12}]$.

Again, using curves fitted to experimental points (see Fig.7) term B was calculated in a similar way. Thus,

when $0 \leq z \leq 4$, $B = -0.3z + 12$, and when $4 \leq z \leq 16$, $B = -\sin[\pi\frac{(z-4)}{12}]$, and finally when $46 \leq z \leq 50$, $B = 0.3(z - 46)$.

Introducing non-dimensional variables,

$h = C_r H$, $x_{cg} = X_{cg} C_r$, $y_{cg} = Y_{cg} C_r$, $z = r_0 Z$, $c = CC_r$

a non-dimensional expression for the air film thickness can be obtained,

$$H = 1 + X_{cg} sin\theta + Y_{cg} cos\theta + C(\theta, Z, \tau) \quad (4)$$

1) corresponding author

Using polar co-ordinate system, mass flow rates involved in the Reynolds' equation can be elaborated as follows:

$$q_\theta = \left(-\frac{h^3}{12\eta}\frac{p}{RT}\frac{\partial p}{r_0 \partial\theta} + \frac{r_0\omega_1}{2}\frac{p}{RT}h\right)\Delta z \tag{5}$$

$$q_z = \left(-\frac{h^3}{12\eta RT}p\frac{\partial p}{\partial z}\right) r_0 \Delta\theta \tag{6}$$

$$q_t = \frac{1}{RT}\frac{\partial(ph)}{\partial t} r_0 \Delta\theta \Delta z \tag{7}$$

Introducing non-dimensional variables,

$h = C_r H, \qquad p = p_a P, \qquad z = r_0 Z, \qquad t = {}^{\tau}/_{\omega_2}$

mass flow rates assume the following non-dimensional forms:

$$q_\theta = \frac{p_a^2 C_r^3}{12\eta RT}\left(-PH^3\frac{\partial P}{\partial\theta} + \Lambda_1 PH\right)\Delta Z \tag{8}$$

$$q_z = \frac{p_a^2 C_r^3}{12\eta RT}\left(-PH^3\frac{\partial P}{\partial Z}\right)\Delta\theta \tag{9}$$

$$q_t = \frac{p_a^2 C_r^3}{12\eta RT}\left(\sigma\frac{\partial(PH)}{\partial\tau}\right)\Delta\theta\Delta Z \tag{10}$$

Where $\Lambda_1 = \frac{6\eta r_0^2\omega_1}{p_a C_r^2}$ and $\sigma = \frac{12\eta r_0^2\omega_2}{p_a C_r^2}$

1) corresponding author

Next task in theoretical calculations was to predict shaft centre motion within the bearing. This was accomplished using non-linear orbit method. Shaft motion in two perpendicular directions is described by the equations given below,

$$m\frac{d^2x_{cg}}{dt^2} = r_0\int_0^b\int_0^{2\pi} p\cos\theta d\theta dz \quad (11)$$

$$m\frac{d^2y_{cg}}{dt^2} = r_0\int_0^b\int_0^{2\pi} p\sin\theta d\theta dz + f_y \quad (12)$$

Where f_y is the force acting on the bearing and given by $f_y = mg\sin\emptyset$ [N].

Using non-dimensional terms, the equations of shaft motion assume the following form:

$$M\frac{d^2X_{cg}}{d\tau^2} = \frac{r_0}{2b}\int_0^{b/r_0}\int_0^{2\pi} P\cos\theta d\theta dZ \quad (13)$$

$$M\frac{d^2Y_{cg}}{d\tau^2} = \frac{r_0}{2b}\int_0^{b/r_0}\int_0^{2\pi} P\sin\theta d\theta dZ + F_y \quad (14)$$

where $F_y = {f_y}/{(2p_a b r_0)}$ is a non-dimensional load on the bearing.

The above equations of motion were solved using Crank-Nicolson numerical procedure.

Utilizing continuity of flow over a unit domain (see Figure 9) and employing finite difference method, pressure distribution within the air film can be calculated. For the case of stationary shaft, convergence limits for the numerical calculations were set as follows:

1) corresponding author

$$\left[\left(p^{n+1} - p^{n}\right) \Big/ p^{n} \right] < 10^{-6} \tag{15}$$

$$\left[\left({x_{cg}}^{n+1} - {x_{cg}}^{n}\right) \Big/ {x_{cg}}^{n} \right] < 10^{-6} \tag{16}$$

$$\left[\left({y_{cg}}^{n+1} - {y_{cg}}^{n}\right) \Big/ {y_{cg}}^{n} \right] < 10^{-6} \tag{17}$$

The case with shaft rotating at speed in instability calculations required only eqn (15).

The flow chart detailing steps taken during calculations is shown in Figure 10.

4. Experimental testing

4.1 Apparatus

Figure 11 schematically presents apparatus used for experimental testing of the bearing with squeeze film ultrasonic levitation. Essential and characteristic feature of the apparatus is the shaft vertically positioned and supported by an aerostatic thrust bearing placed on the base plate. This apparatus was especially designed and built to experimentally determine the load capacity of the bearing and its dynamic stability when it operates at speed with and without squeeze film ultrasonic levitation. Shaft made of stainless steel had nominal diameter of 30 mm and was fitted into the bearing with three different radial clearances stated earlier. Thrust bearing supporting the shaft and ensuring that it freely floats in the direction of its main axis

1) corresponding author

was fed with compressed air supplied from an external source. Running of the shaft at speed was provided by an air turbine consisting of buckets machined at one end of the shaft and three air nozzles fixed to the housing and supplying air jets tangent to the shaft's circumference. Operation of PZTs and therefore the journal bearing tested was controlled by an amplifier and frequency generator. A schematic diagram showing components of the control system is presented in Figure 12. Position of the shaft within the journal bearing was measured in two planes by contactless sensors. The apparatus was magnetically clamped to the base plate and could be tilted by desired angle ϕ creating, in consequence, a loading on the bearing in a controlled way (see Fig. 12). The load on the bearing was calculated from the equation $f_y = mgsin\emptyset$ [N] introduced earlier.

Central objective of experimental testing was to determine the effect of squeeze film ultrasonic levitation on the dynamic stability of the bearing when it was running at speed. Additionally, information concerning load capacity of the bearing was also looked for.

4.2 Procedure

Testing began by setting offset voltage, V_{off} , which produced constant displacement of the PZTs and hence the initial elastic deformation of the bearing. Vibration displacement (amplitude) resulting in a cyclic elastic deformation of the bearing was controlled by the running voltage V_{amp}. In the experiments reported here V_{off} was usually set to 70 V and V_{amp} to 60 V.

Procedure for a typical test was as follows. First, it was required to ensure that the shaft was in true vertical position and floated freely on air cushion created by the

1) corresponding author

aerostatic bearing fitted into the base of testing apparatus. Next, the offset voltage of 70 V was set so that the PZTs expanded and the bearing deformed accordingly. Following that, running voltage, corresponding to the amplitude of cyclic elastic deformations of the bearing, equal to 1.5 μm, was adjusted to 60 V. As a result of rapid cyclic deformations of the bearing with the frequency of 58.3 kHz used throughout experimental testing an air film was created separating shaft from the bearing due to the squeeze mechanism. For the stationary shaft, load carrying capacity of the air film created by SFUL was ascertained by gradual tilting of the test apparatus base thus increasing the load on the bearing and monitoring its clearance with a non-contact probe.

After ensuring that SFUL creates a pressure in the air film able to support a load even for the stationary shaft, running tests were carried out. Firstly, stability of the bearing running without SFUL was determined by measuring shaft's displacement in two planes for a given radial clearance and the load on the bearing. These data enabled construction of diagrams illustrating movement of the shaft's centre within the bearing. The form the shaft's centre path provided information whether operation of the bearing was stable or not at a certain rotational speed. In a similar way, stability of the bearing running with SFUL was determined.

5. Results and their discussion

Load capacity of the bearing resulting from SFUL alone (stationary shaft case) is shown in Figure 13. In this figure experimentally measured load capacity for three different radial clearances is compared with calculated load capacities. Frequency of bearing elastic deformation was fixed for all cases at 58.3 kHz. Vertical axis

1) corresponding author

represents a distance between the shaft and bearing as measured by contactless probe while horizontal axis depicts corresponding load on bearing. It can be observed that the bearing with stationary shaft is able to support a load of up to 5.5 N at which separation of the shaft from bearing is almost non-existent. Furthermore, reasonably good agreement between measured and calculated load capacities can be discerned. Additional observation is an evident contribution of radial clearance to the load capacity of the bearing.

Dynamic behaviour of the bearing is best judged by the path traced by the shaft centre. Figure 14 shows calculated movement of the shaft centre for the bearing without SFUL. Figure 14a depicts the case of stable running of the bearing at 200 rpm with the load on the bearing equal to 0.2 N and radial clearance of 10 μm. Figure 14b is for unstable running of the same bearing at 300 rpm. This observation is further supported by more detailed plots (drawn in magnification) showing that for stable running case (200 rpm) the motion of the shaft centre has converging tendency (see Fig. 14c) while the unstable running is characterised by the opposite behaviour of the shaft (see Fig. 14d).

Calculated results for stable and unstable running of the bearing with SFUL are shown in Figure 15. Hence, Figure 15a illustrates shaft centre motion during stable running at 9000 rpm with the load on the bearing equal to 0.2 N and 10 μm radial clearance. The unstable running of the bearing under the same load and with the same radial clearance was calculated to occur at 10,000 rpm and is depicted in Figure 15b. Further elaboration of the stable and unstable running is provided by magnified plots of the motion of shaft centre (see Figures 15c and 15d). Stable running at 9000 rpm is exemplified by converging tendency of the shaft centre

1) corresponding author

motion while unstable running at 10,000 rpm is characterised by diverging motion tendency.

Experimentally determined motions of the shaft centre for the bearing operating with SFUL are depicted in Figure 16. It was found that the bearing can stably run at the speed of 9000 rpm. The evidence for that is provided by Figure 16a in which movement of the shaft centre is depicted. It can be clearly noticed that the locus of the movement of shaft centre is very compact- not exceeding 1 μm. This is an excellent testimony to the beneficial effect of SFUL on dynamic stability of the bearing. Comparing that result to the speed at which stable running of the bearing without SFUL was possible (200 rpm) it is justified to infer that the stabilizing effect provided by SFUL is very considerable indeed. The threshold speed at which bearing running with SFUL was found to become unstable is equal to 13,200 rpm. This is illustrated by Figure 16b in which the locus of shaft centre movement is seen to grow. It is worthwhile mentioning that experimentally measured threshold speed of instability is greater than that predicted by calculations. This discrepancy might be attributed to some simplifications assumed during the construction of bearing's computer model.

6. Conclusions

Results of numerical calculations and experimental measurements presented in this paper enable drawing the following conclusions.

1. Results testify to the practical feasibility of the concept of a journal air bearing utilizing squeeze film ultrasonic levitation (SFUL) especially where required load capacity is low and operating environment calls for extreme cleanliness, compact design, and energy efficiency.

1) corresponding author

2. Squeeze film ultrasonic levitation proved to be a powerful factor improving dynamic stability of an air bearing running at speed under very light load.

3. Lightly loaded air journal bearing considered to be inherently unstable can have threshold speed of instability increased many times by incorporating SFUL into its design and operation.

4. Bearing used in the studies presented here had its instability speed increased more than thirty times by the use of squeeze film ultrasonic levitation.

7. References

[1] V. Vandaele, P. Lambert, A. Delchambre, Non-contact handling in micro-assembly: Acoustical levitation, Precision Engineering, 29 (2005) 491-505.

[2] T. A. Stolarski, Numerical modelling and experimental verification of compressible squeeze film pressure, Tribology Interntional, 43 (1–2) (2010) 356–360.

[3] T. A. Stolarski and Wei Chai, Self-levitating air contacts, Int. J. Mech. Sci., 48 (2006) 601-620.

[4] T. A. Stolarski and Wei Chai, Load-carrying capacity generation in squeeze film action, Int. J. Mech. Sci., 48 (2006) 736-741.

[5] T. A. Stolarski and Wei Chai, Inertia effect in squeeze film air contact, Tribology International, 41(2008) 716-723.

[6] E. O. J. Salbu, Compressible squeeze films and squeeze bearings, J. Basic Eng., 86 (1964) 355-366.

[7] L. F. Warnock, Dynamic gas film supported inertial instrument, US Patent No. 3339421 (1967).

[8] T. B. R. Farron, Squeeze film bearings, US Patent No. 3471205 (1969).

[9] C. L. Emmerich, Piezoelectric oscillating bearing, US Patent No. 3351393 (1967).

1) corresponding author

[10] R. A. Scranton, Planar and cylindrical oscillating pneumato-dynamic bearings, US Patent No. 4666315 (1987).

[11] M. Wiesendanger, Squeeze film air bearing using piezoelectric bending elements, PhD thesis, Ecole Polytechnique Federale de Lausanne (2001).

[12] D. N. Ha, T. A. Stolarski, S. Yoshimoto, An aerodynamic bearing with adjustable geometry and self-lifting capacity, Proc. IMechE, part J, Journal of Engineering Tribology, 219 (2005) 33-39.

[13] S. Yoshimoto, H. Kobayashi, M. Miyatake, Float characteristics of a squeeze-film air bearing for a liner motion guide using ultrasonic vibration, Tribology International, 40 (2007) 503-511.

[14] Y. Ono, S. Yoshimoto, M. Miyatake, Impulse-Load Dynamics of Squeeze Film Gas Bearings for a Linear Motion Guide, J. Tribol. 131 (2009) 041706.

[15] Y. Xue, T. A. Stolarski, S. Yoshimoto, Air journal bearing utilizing near field acoustic levitation - stationary shaft case, Proc. IMechE, part J, Journal of Engineering Tribology, 225 (2011) 20-127.

1) corresponding author

Figure1

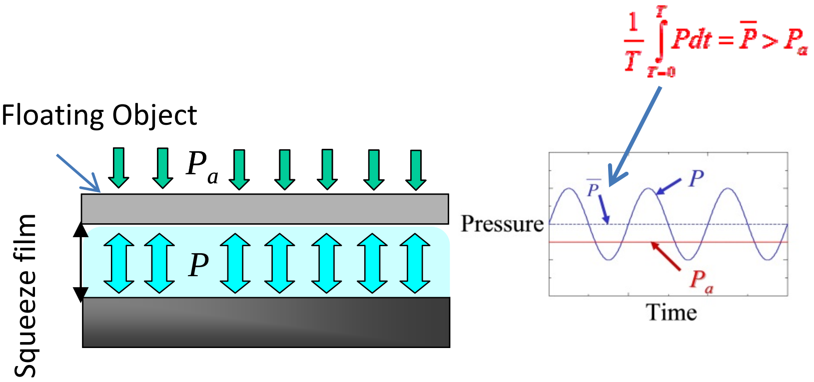

Figure 1

Figure2

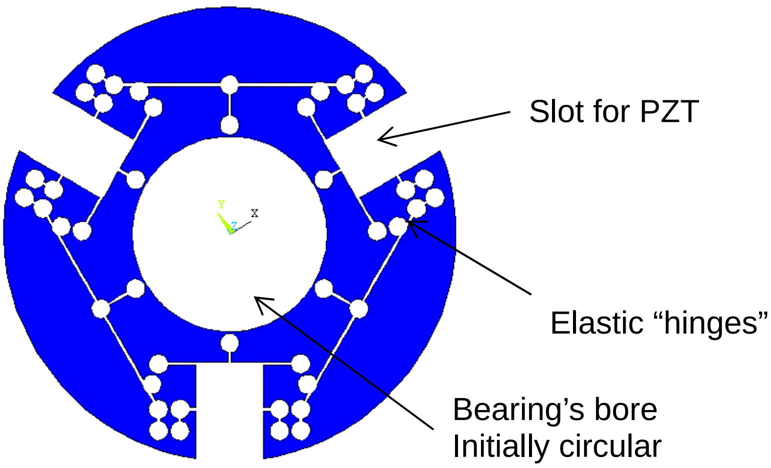

Figure 2

Figure3

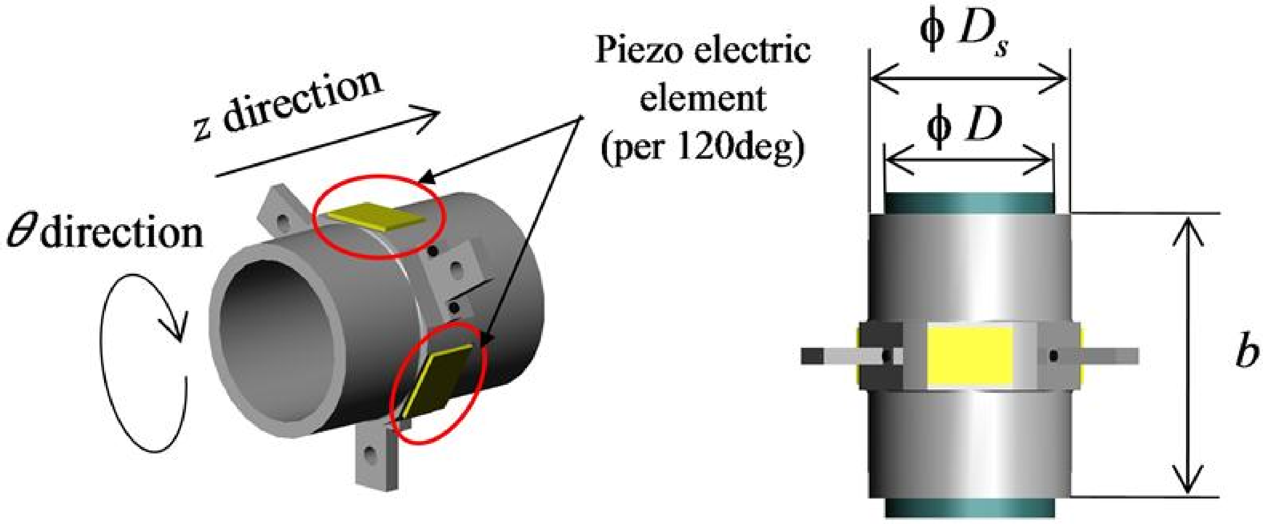

Figure 3

Figure4

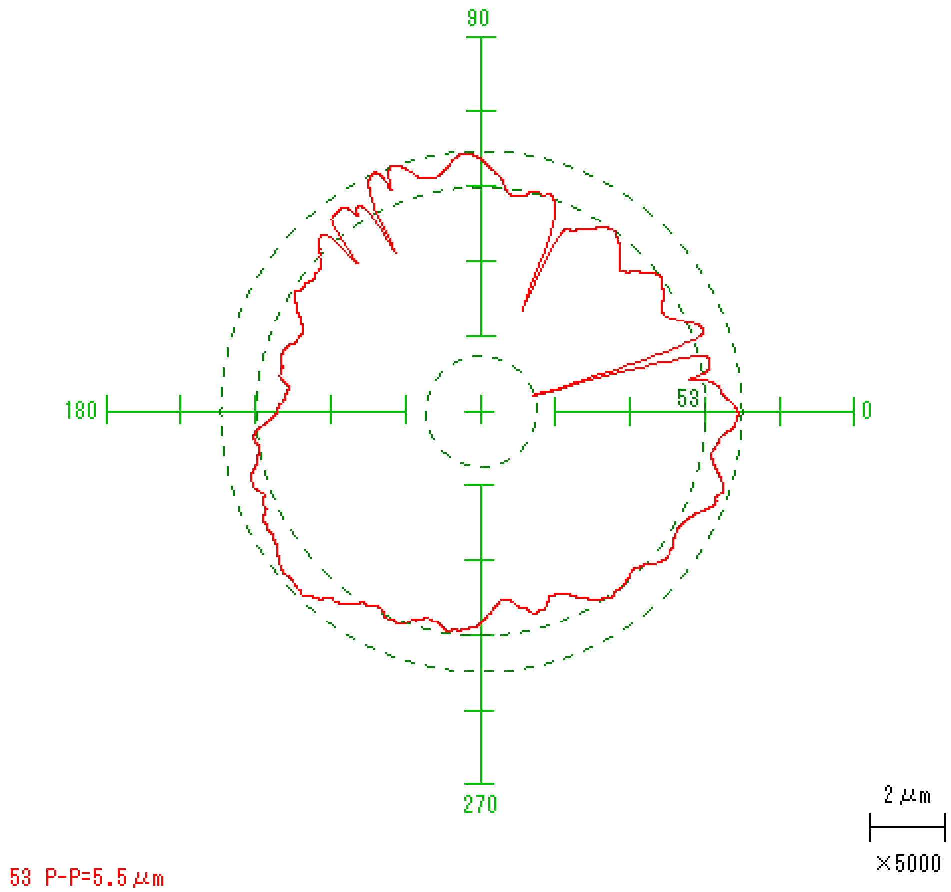

Figure 4

Figure5

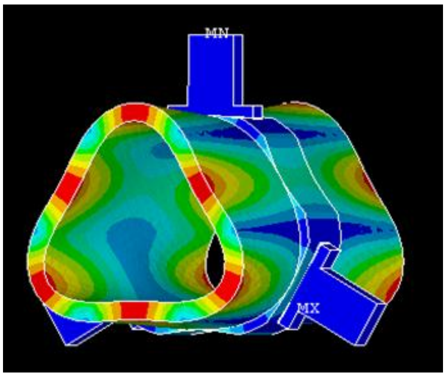

(a) 21.6 kHz

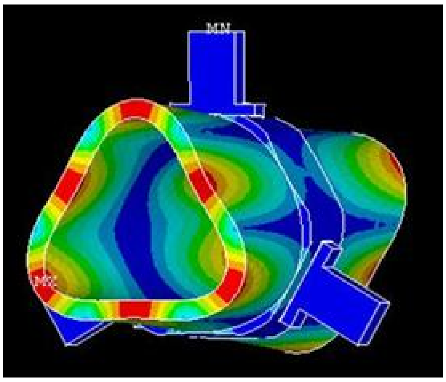

(b) 21.8 kHz

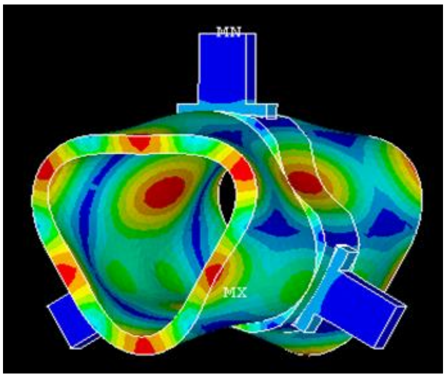

(c) 33.3 kHz

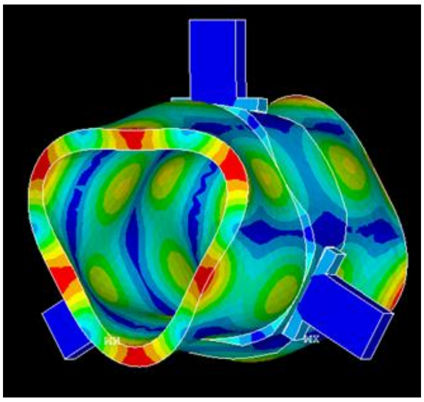

(d) 43.1kHz

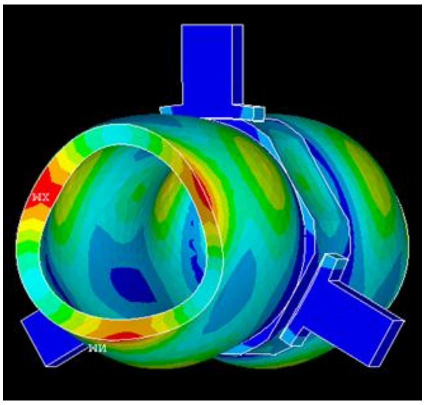

(d) 58.2 kHz

Figure 5

Figure6

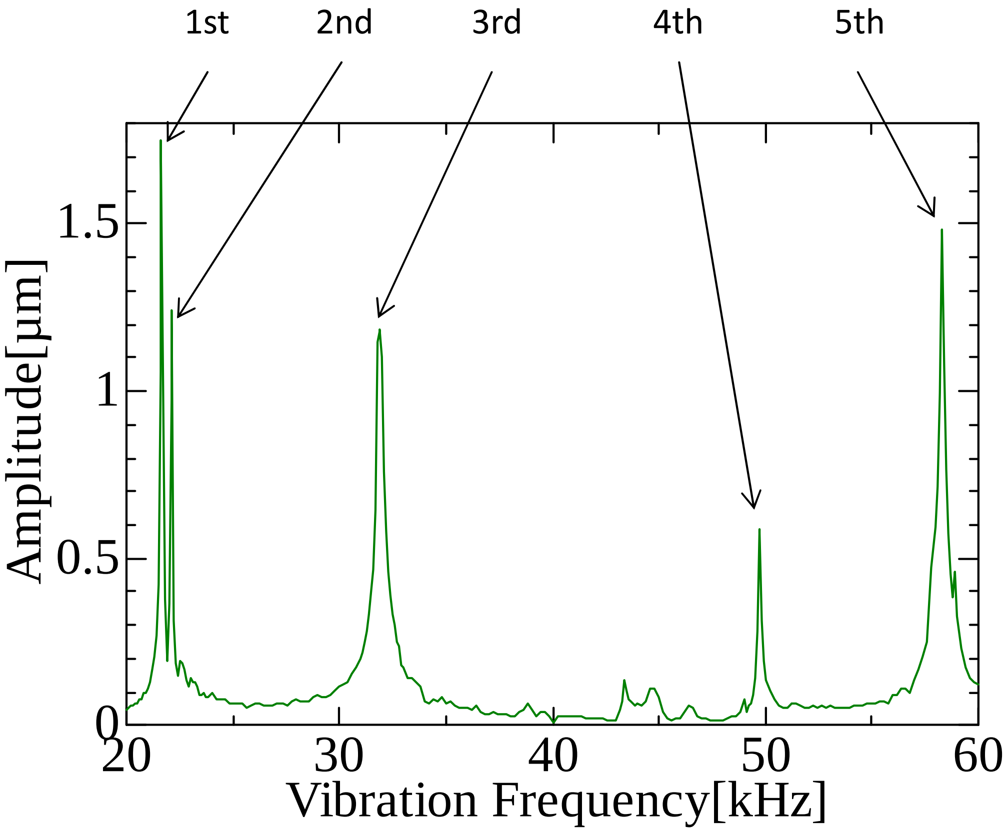

Figure 6

Figure7

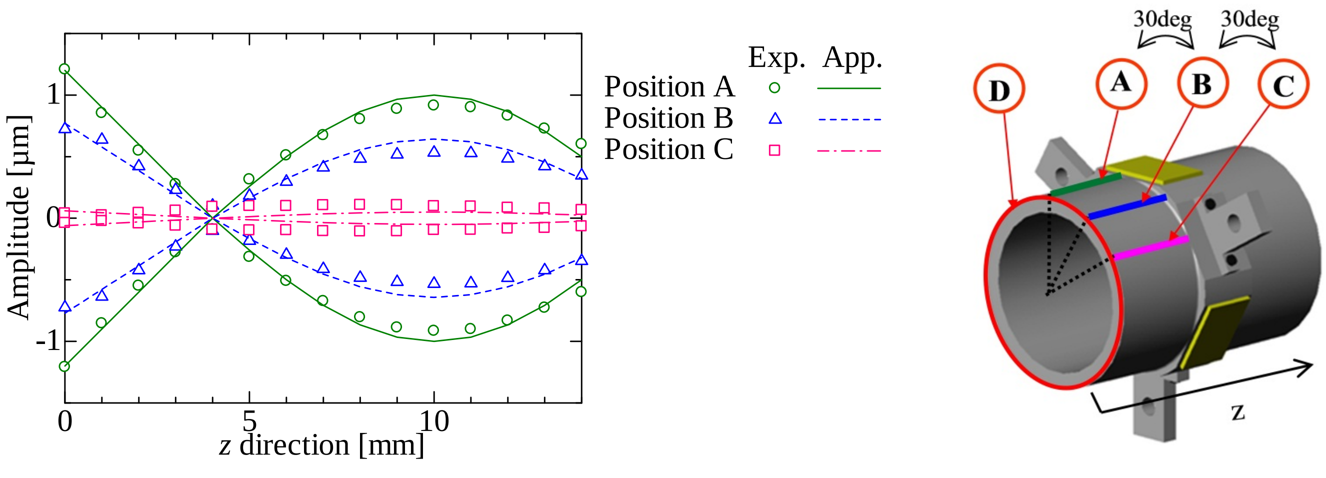

(a)

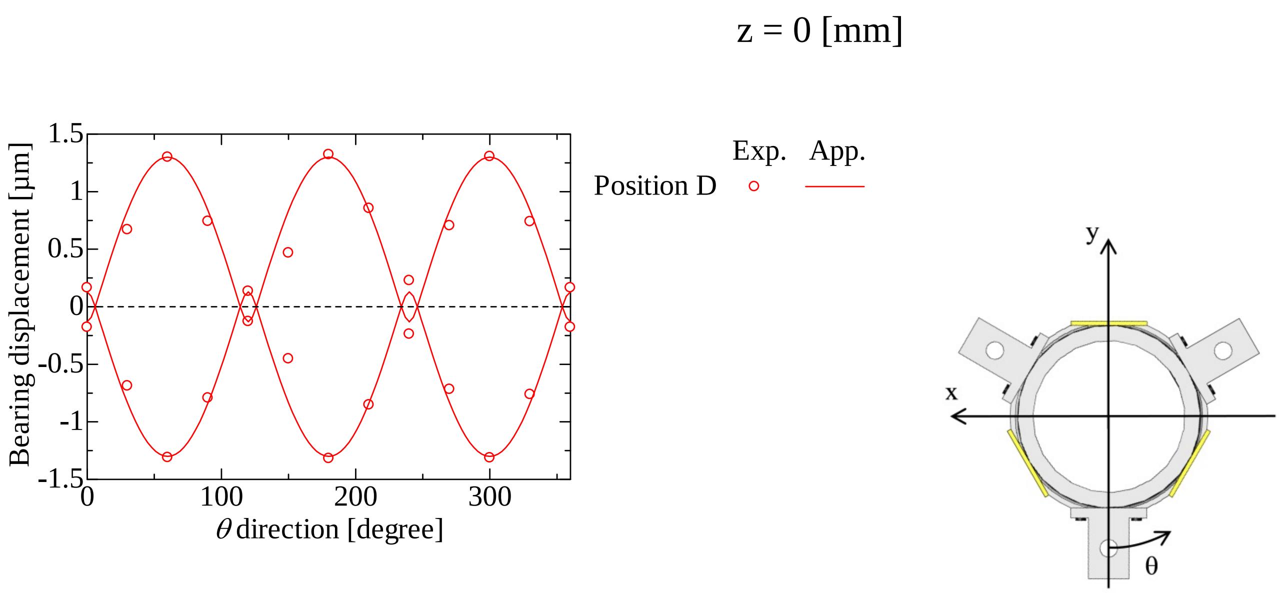

(b)

Frequency of vibration – 58.3 kHz

(5^{th} mode of elastic deformation)

Figure 7

Figure8

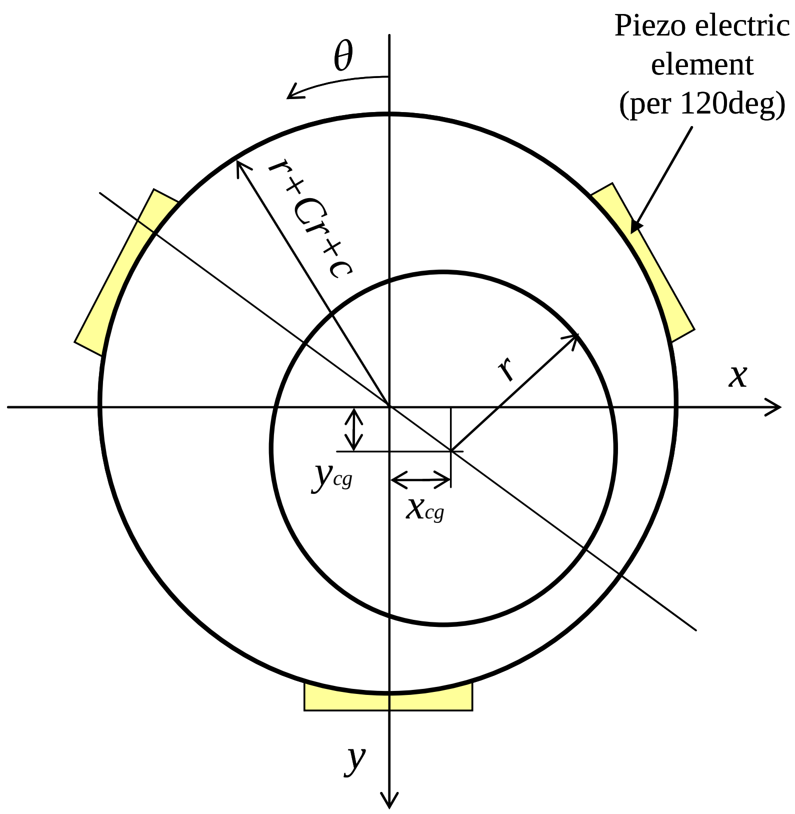

Figure 8

Figure9

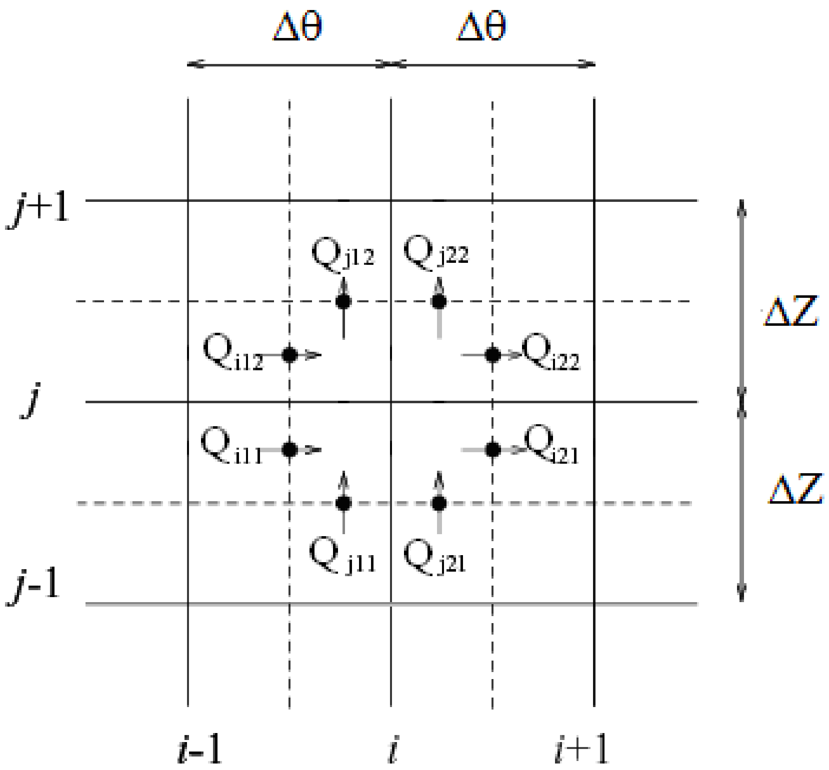

Figure 9

Figure10

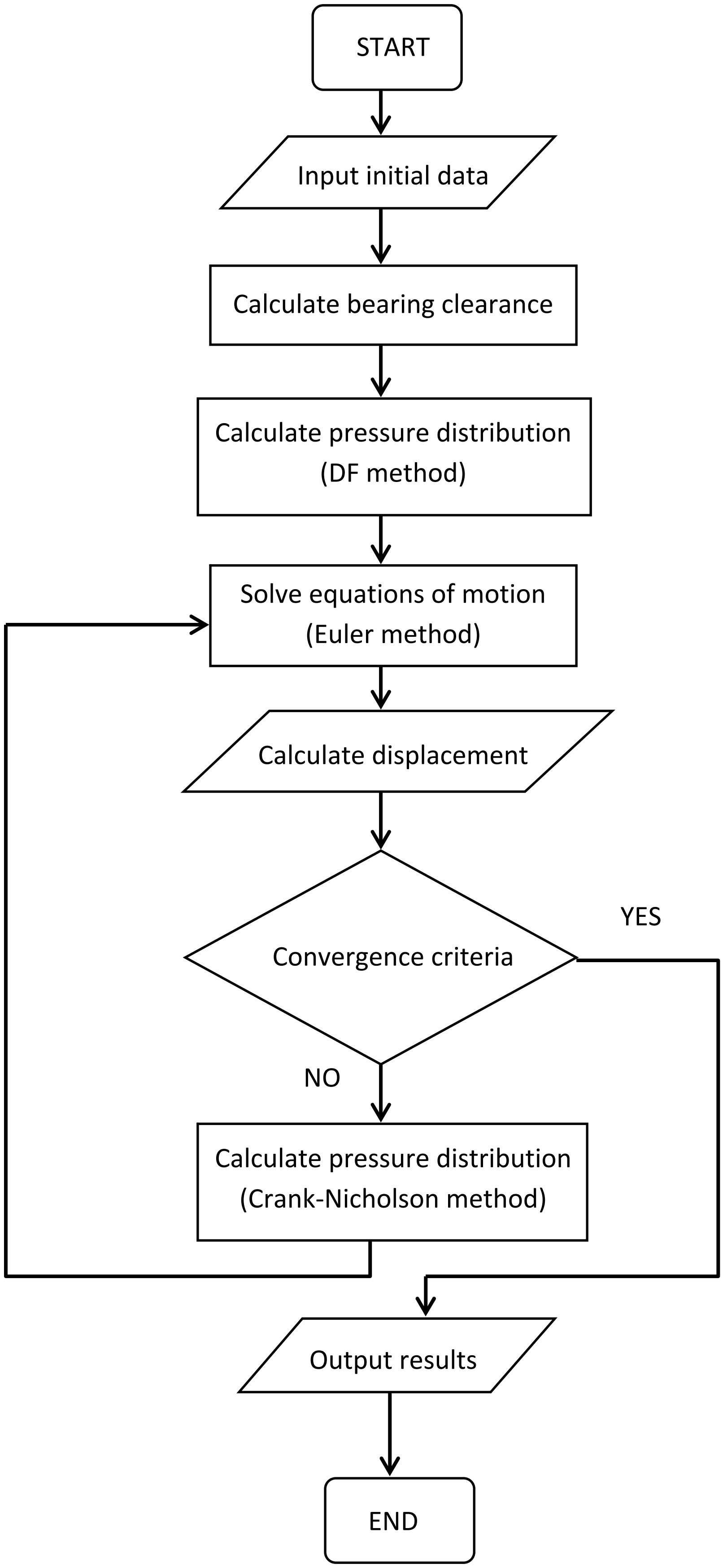

Figure 10

Figure11

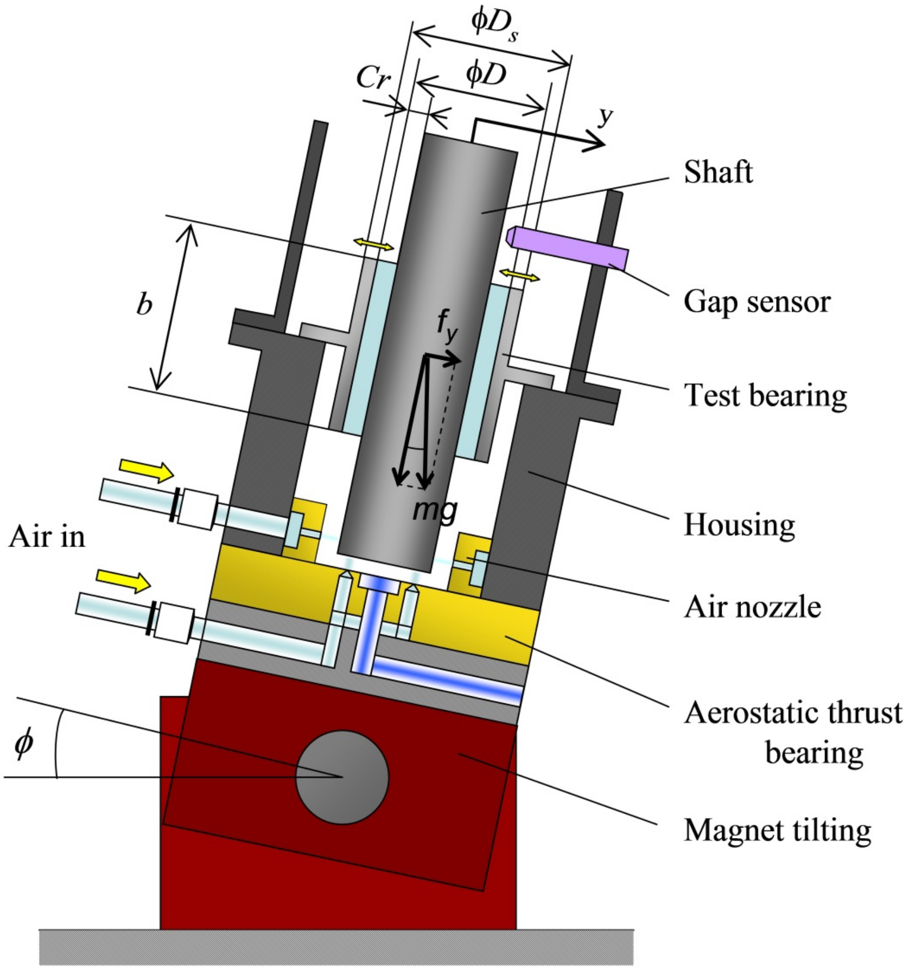

Figure 11

Figure12

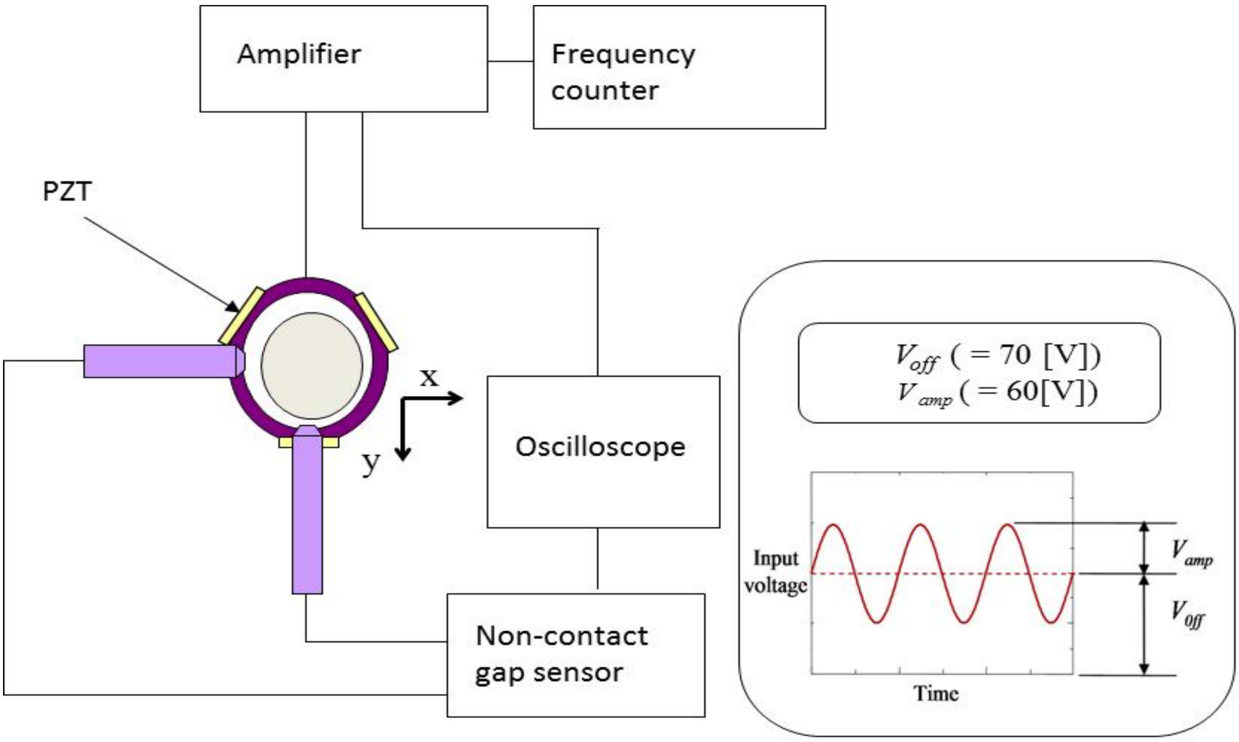

Figure 12

Figure13

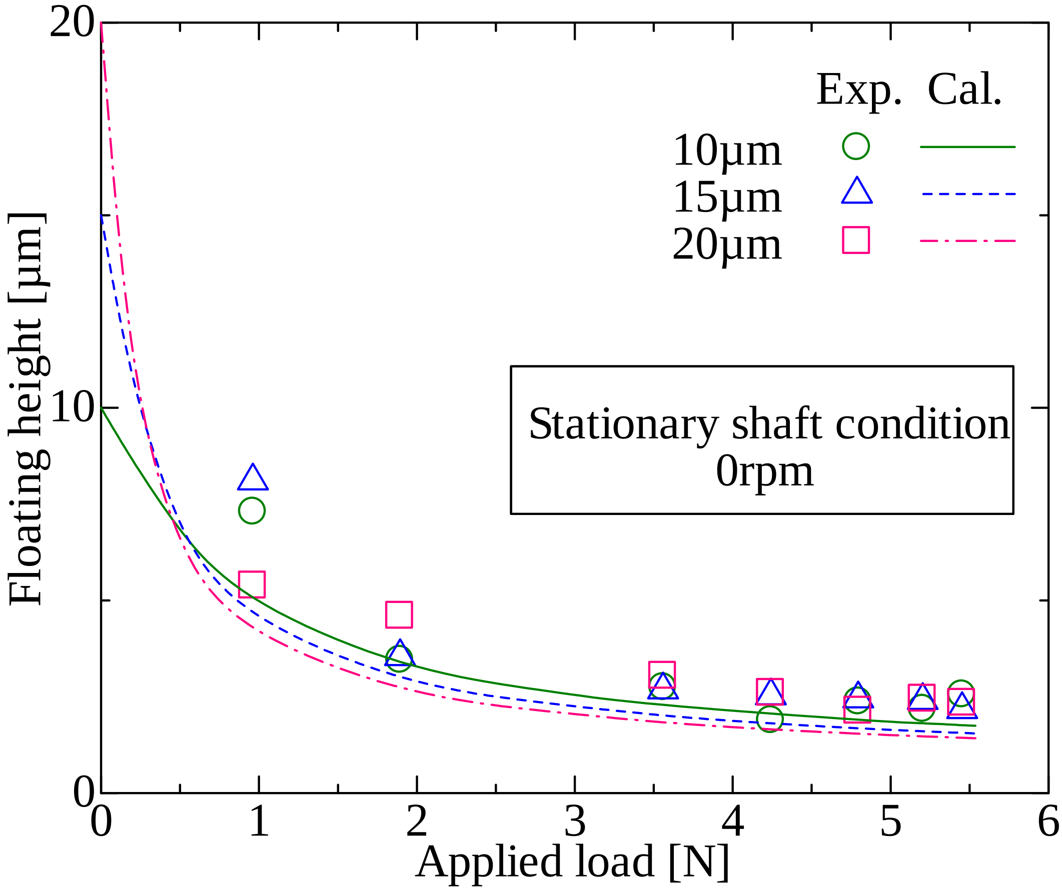

Figure 13

Figure14

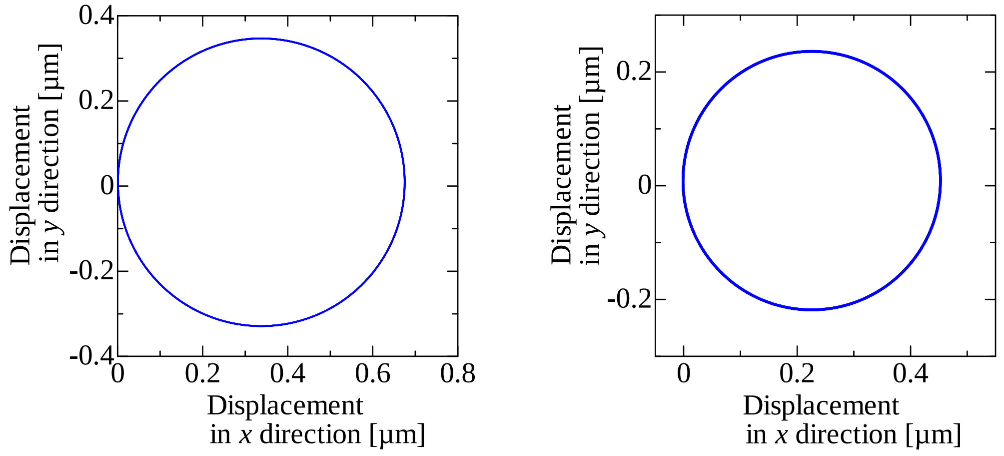

(a) 200 rpm (STABLE)

(b) 300 rpm (UNSTABLE)

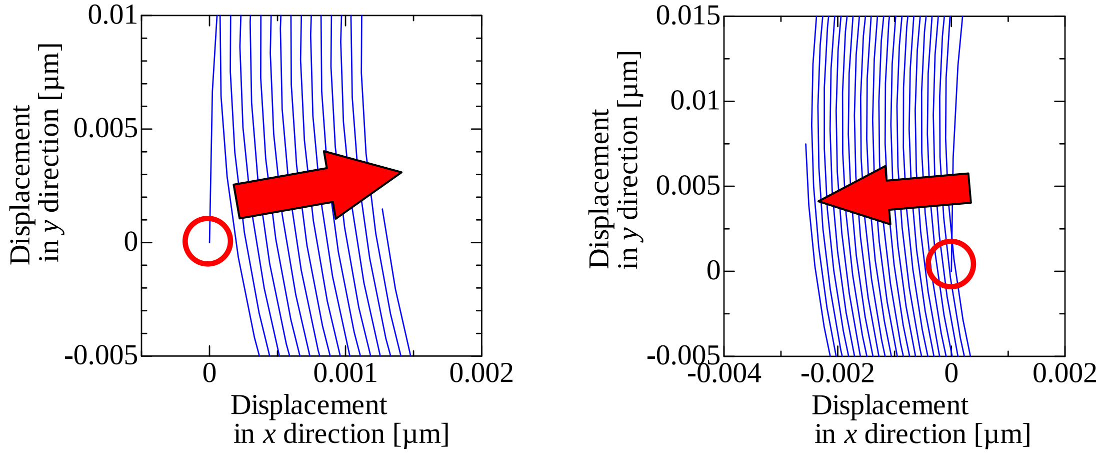

(c) 200 rpm (STABLE)

(d) 300 rpm (UNSTABLE)

Figure 14

Figure15

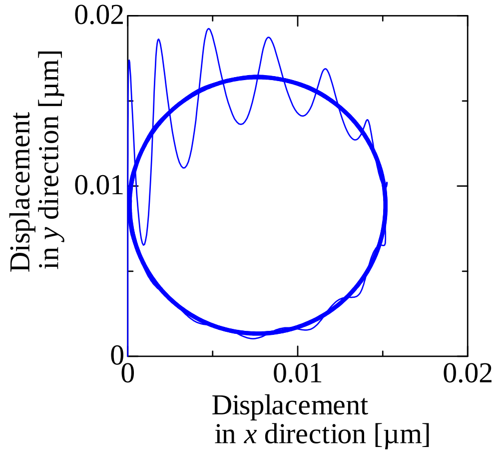

(a) 9000 rpm (STABLE)

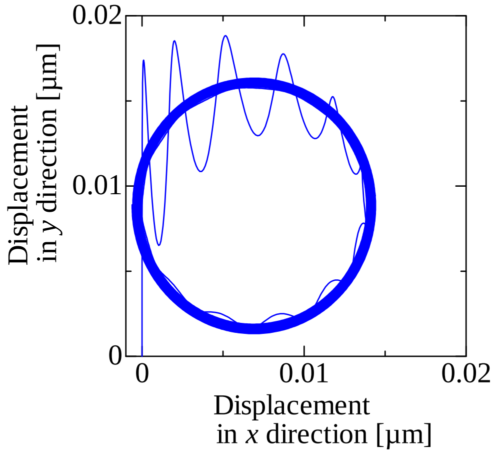

(b) 10,000 rpm (UNSTABLE)

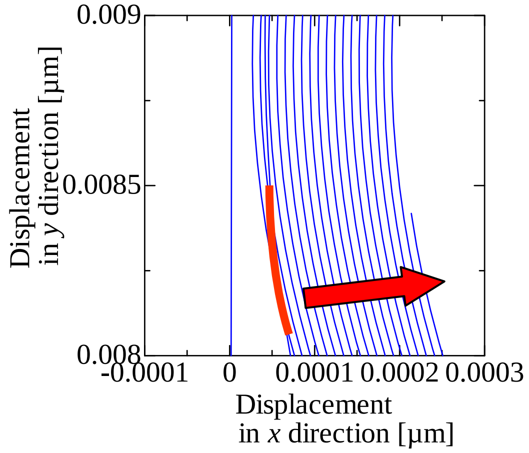

(c) 9000 rpm (STABLE)

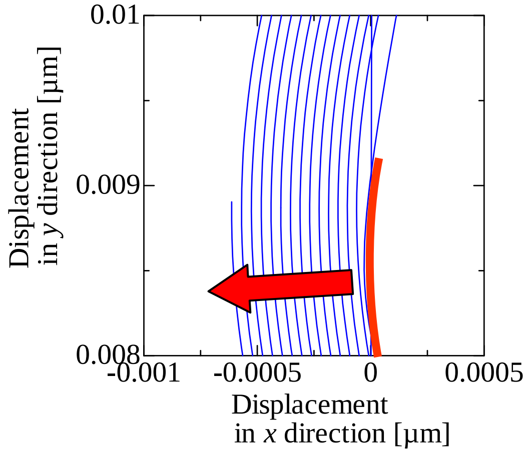

(d) 10,000 rpm (UNSTABLE)

Figure 15

Figure16

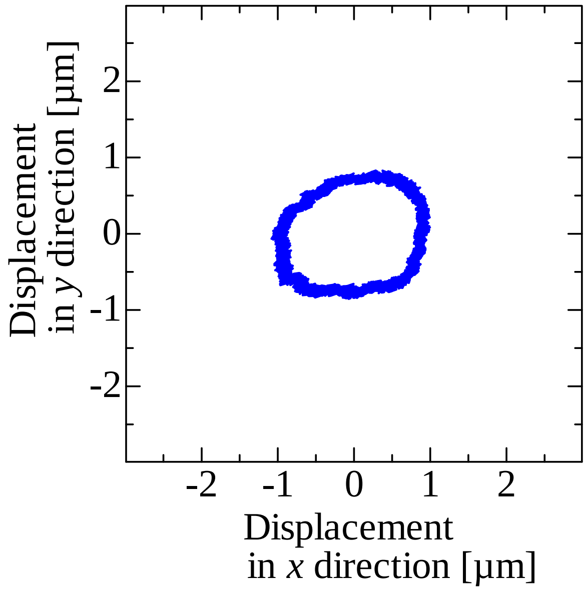

(a) 9000 rpm (STABLE)

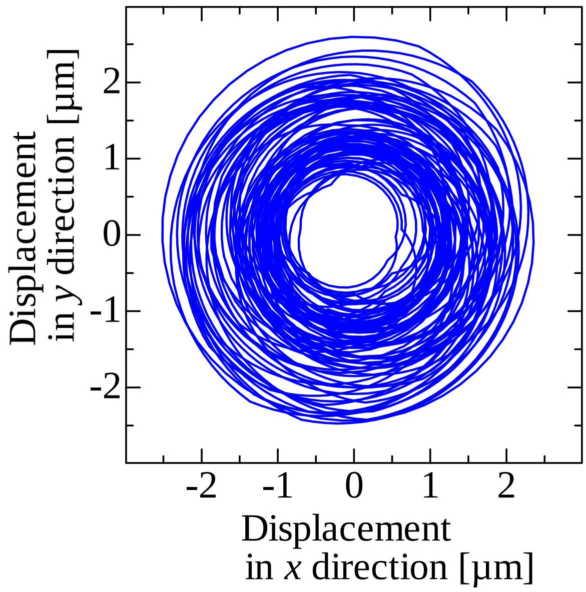

(b) 13,200 rpm (UNSTABLE)

Figure 16

Table1

Outside diameter [mm]	36
Nominal inside diameter [mm]	30
Wall thickness [mm]	3
Radial clearance used[mm]	0.01; 0.015; 0.02
Bearing's length [mm]	50
Shaft length [mm]	103
Shaft mass [kg]	0.565

Table 1